

**DEVELOPMENT OF A HIGH TEMPERATURE THIN FILM  
STATIC STRAIN GAGE**

Charles O. Hulse and Richard S. Bailey  
United Technologies Research Center  
East Hartford, Connecticut

and  
Howard P. Grant and John S. Przybyszewski  
Pratt & Whitney Division  
East Hartford, Connecticut

The objective of this effort is to develop a new thin film resistance strain gage system which will be suitable for use inside gas turbine engines on blades or vanes at temperatures up to 1250 K. These gages are to be capable of making strain measurements to  $\pm 2000$  microstrain with total errors of no more than  $\pm 10$  percent during a 50 hour period. In addition to survival and stability in this hostile environment, attaining a low temperature coefficient of resistance, of the order of 20 ppm/K or less, is an important goal. This requirement arises from the presently unavoidable uncertainties in the measurement of exact temperatures inside gas turbine engines for use in making corrections for apparent strain.

**SENSOR PROPERTIES**

The most desirable material to select as a strain sensitive resistor would be a pure, precious metal which would have a high melting point and be inert to oxidation attack. Unfortunately, the resistances of pure metals all have high thermal sensitivities to temperature which is unacceptable in this application. Unacceptably large uncertainties in strain (errors) result when high coefficients of resistance are combined with the typical uncertainties in measurements of the temperature of gas turbine parts. This consideration is further complicated when the sensor must be used on a structure containing a high thermal gradient.

Alloying with other precious metals to form solid solutions can be used to introduce electron scattering centers whose concentrations and resistance effects are essentially independent of temperature. Unfortunately, the choices available do not result in alloys whose resistivities have sufficiently low thermal sensitivities to be

---

\*Work done under NASA Contract NAS3-23722

useful. The optimum sensor composition developed in this and previous programs (refs. 1-4) is an alloy of Pd containing 13 weight percent Cr. This alloy is particularly desirable because, not only does the Cr act as effective scattering agent to increase the resistance and lower the thermal sensitivity of resistance of the alloy, but the Cr diffuses to the surface to form a coating of  $\text{Cr}_2\text{O}_3$  which resists further oxidation of the Cr. Figure 1 shows the resistance versus temperature behavior of this alloy. The fact that the resistance is linear with temperature indicates that the Cr remains in complete solid solution over the full temperature range of interest and that no ordering effects occur.

Unfortunately, when this alloy is prepared as a sputtered film only 6.5 micrometers thick, the amount of Cr in the film is not sufficient to form a protective coating without almost completely depleting the remaining alloy of Cr. Figure 2 shows how the resistance of different thicknesses of the PdCr alloy changes with time when exposed to oxidation at 1250 K.

### PROTECTIVE OVERCOATS

Efforts are currently underway to develop protective overcoat/top seal coatings to overcome this oxidation problem. Alumina has been selected as the primary overcoat material because of the general recognition that it forms the most oxidation resistant coatings for use on nickel-base superalloys. Unfortunately, sputtered films of alumina do not remain completely dense and inert upon firing to elevated temperature for various reasons: (a) the transformation from gamma to alpha or from amorphous to crystalline, (b) evolution of argon entrapped in the structure during sputtering, (c) oxidation to restore stoichiometry, and (d) accommodation of the strains caused by the differences in thermal expansion between the alumina and the superalloy substrate, which are typically of the order  $7 \times 10^{-6}/\text{K}$ . Table I presents a listing of the various top seal coats which are being evaluated in attempts to make the alumina impervious to oxygen.

Preliminary experiments are also underway to evaluate the potential advantages of sputtering the alumina films on a heated substrate. Because these films will be formed at a high temperature they should have a high stress free temperature and experience only moderate tensile stresses when heated to the highest temperature of use.

### INSULATION COATINGS

Decreases in the measured resistances of strain gage circuits can also occur because of electrical leakages through the alumina insulation coating on the Hastelloy-X substrate. These create additional parallel paths for current to flow through the metal substrate. Figure 3 shows an example where shorting has developed at high temperatures which gradually became worse with time. Measure-

ments of the resistance between the gage and the substrate can be used to confirm the cause of this behavior.

Our investigations of this problem have focused on the importance of surface defects originally present on the highly polished metal surface and debris present on these surfaces during sputtering. These defects can result in abnormal growths in the sputtered films which tend to become detached during subsequent thermal cycling to form very fine pinholes. We have carried out careful examinations of all of our sputtered surface to ensure that these sources are removed, and we feel that our further results will confirm that most of this problem can be avoided by the use of these careful procedures.

## TEMPERATURE COMPENSATION AND LEAD WIRE CONSIDERATIONS

### Temperature Compensation Design

An analysis of temperature effects on static strain gage accuracy carried out by NASA and UTC during Task 1 and 2 of the program concluded that active temperature compensation would be needed in addition to corrections for residual apparent strain due to temperature. Active resistive temperature compensation can be accomplished by installing an additional temperature sensitive (relatively strain insensitive) element at the point of measurement, and combining the output signal from this element with the output signal from the strain gage element, as shown in Figure 4. Good thermal compensation can be expected over only a moderate temperature range because the thermal sensitivities of the gage and the compensating element typically vary differently with temperature. Note that the use of an adjustable resistor across the compensating arm of the bridge (the dashed lines in Figure 4) as a means of further adjusting the compensation, is not advisable because this shunt would also be across two of the three lead wire resistances, and therefore would defeat the lead wire cancellation provided by the 3-wire hookup.

### Lead Resistance Effects

Once the strain gage bridge adjustments in Figure 4 have been set for initial balance, including the temperature compensation adjustments, subsequent changes in temperature distribution in the lead wires and lead films can produce apparent strain due to temperature at the bridge output in two ways: (a) common mode changes in all lead resistances, and (b) differential changes due to transverse temperature gradients. In order to reduce the common-mode error to an acceptable level, the temperature compensation element in the bridge of Figure 4 must have a resistance and temperature coefficient of resistance that produce the same total level of change in resistance with temperature as the strain element, within about 5%. Only if this is true can the bridge ratio be set close to 1:1 as required to minimize this type of error. The effects of temperature gradients can be minimized by routing the two critical leads as close together as possible.

## Lead Wire Thermocouple Effects

For a gage factor of 2 and for a bridge voltage  $E_1$  of 5 volts, the thermocouple effect in any arm of the bridge is about 1 microstrain for every 5 microvolts of stray thermocouple emf. The thermocouple emf generated in each lead wire, lead film, strain element, or compensating element is proportional to the temperature difference between the two ends of the element. Factors of proportionality (thermocouple emf per Kelvin, relative to platinum measuring leads) are listed in Table II for several candidate metals and alloys. These factors range from  $-15 \mu\text{v/K}$  to  $+32 \mu\text{v/K}$  so that careful attention must be used in choosing materials and layout.

Thermocouple effects can be reduced if the bridge voltage  $E_1$  is increased, but  $E_1$  must not be made so large that significant self-heating of the strain element occurs. Thermocouple effects may also be reduced by employing pulsed DC excitation to raise  $E_1$  by an order of magnitude without producing self-heating. Capacitively and inductively coupled transient noise voltages are potential problems when pulsed excitation is employed. In principle, residual thermocouple effects on static strain measurements can also be completely suppressed by turning off the bridge excitation before each strain measurement and readjusting a bucking voltage to rebalance the bridge.

## SUMMARY AND CONCLUSIONS

The Pd-13 Cr (weight percent) alloy developed in this program appears to meet the program goals of stability and reproducibility for use as a static strain gage up to 1250 K when prepared in bulk form. When prepared as a 6.5 micrometer thick sputtered strain gage, however, the naturally occurring protective coating of  $\text{Cr}_2\text{O}_3$  is inadequate to prevent oxidation attack and a protective overcoat/seal coat system is required. An evaluation of these systems is currently underway as well as an examination of the use of sputtering at elevated temperature to reduce the problems caused by the differences in thermal expansion between the substrate and sputtered alumina layers.

The important factors and problems involved in the selection and use of lead wires with static strain gages have been reviewed. It is believed that problems with electrical leakage between the strain gage and the substrate can be overcome primarily by the use of extreme care in surface preparation before sputtering to eliminate surface defects which can cause defects to occur in the sputtered layers. This is also still being evaluated.

## REFERENCES

1. Hulse, C. O.; Bailey, R. S.; and Lemkey, F. D.: High Temperature Static Strain Gage Alloy Development Program, NASA CR-174833, March 1985.
2. Hulse, C. O.; Bailey, R. S.; and Grant, H. P.: The Development of a High Temperature Static Strain Gage System. Turbine Engine Hot Section Technology, 1985. NASA CP-2405, pp. 45-49.
3. Hulse, C. O.; Bailey, R. S.; and Grant, H. P.: Development of a High Temperature Static Strain Sensor. Turbine Engine Hot Section Technology, 1986. NASA CP-2444, pp. 85-90.
4. Hulse, C. O.; Bailey, R. S.; Grant, H. P.; and Przybyszewski, J. S.: High Temperature Static Strain Gage Development Contract, NASA CR-180811, July 1987.

TABLE I. STRAIN GAGE OVERCOAT SYSTEMS

<u>Type</u>	<u>Sensor PdCr</u>	<u>Sputtered</u>					<u>Transfer tape Glass</u>
		<u>Al<sub>2</sub>O<sub>3</sub></u>	<u>FeCrAl</u>	<u>Pt</u>	<u>Glass</u>	<u>Al</u>	
1	X	X					
2	X	X	X				
3	X	X		X			
4	X	X			X		
5	X	X				X	
6	X	X					X

TABLE II. APPROXIMATE PROPERTIES OF SELECTED METALS AND ALLOYS

Material	Compo- sition Weight Percent	TC EMF Relative To Platinum 273 K to 1250 K ( $\mu\text{V/K}$ )	Melting Point (K)	Temp. Coeff. Lin. Exp. 273 K to 1250 K ( $\text{K}^{-1}$ ) $\times 10^6$	Temp. Coeff. of Resistance $\alpha$ ( $\text{K}^{-1}$ )	Resis- tivity $\rho$ (ohm-cm)	Product $\alpha\rho$ (ohm-cm $\cdot\text{K}^{-1}$ )	Gage Factor G	Ratio $\alpha/G$ ( $\text{K}^{-1}$ )	Lead Wire Resistance for 1 meter of .25 cm Wire $R_w$ ( $\times 10^6$ ) $\rho$ (ohms/meter)
Palladium	Pd	-15	1827K	12	.003800	$10.8 \times 10^{-6}$	$.041 \times 10^{-6}$	6.6	.000576	2.2
Nickel	Ni	-12	1608K	13	.004800	$10 \times 10^{-6}$	$.048 \times 10^{-6}$	2.0	.002400	2.0
Alumel	Ni-2Al- 3Mn-1Si	-9	1673K		.001900	$29 \times 10^{-6}$	$.055 \times 10^{-6}$	2.0	.000950	5.8
Platinum	Pt	0	2046K	10	.003000	$10.6 \times 10^{-6}$	$.032 \times 10^{-6}$	4.8	.000625	2.1
Gold	Au	+8	1336K	14	.003400	$2.4 \times 10^{-6}$	$.008 \times 10^{-6}$	2.0	.001700	.48
Aluminum	Al	+9	933K	24	.004000	$2.7 \times 10^{-6}$	$.011 \times 10^{-6}$			
Pd-13Cr	Pd-13Cr	+19*			.000170	$100 \times 10^{-6}$	$.017 \times 10^{-6}$	1.8	.000094	20.0
Pt-10Rh	Pt-10Rh	+10	2100K		.001700	$18 \times 10^{-6}$	$.031 \times 10^{-6}$	2.0	.000850	3.6
Pt-10Ni	Pt-10Ni	+15	1920K		.001400	$30 \times 10^{-6}$	$.042 \times 10^{-6}$	2.0	.000700	6.0
Copper	Cu	+18	1356K	16	.003900	$1.7 \times 10^{-6}$	$.007 \times 10^{-6}$	2.0	.001950	.34
Nichrome	Ni-20Cr	+23	1673K	14	.000100	$108 \times 10^{-6}$	$.011 \times 10^{-6}$	2.0	.000050	21.6
Chromel P	Ni-10Cr	+32	1700K		.000320	$70 \times 10^{-6}$	$.022 \times 10^{-6}$	2.0	.000160	14.0
Ni-30Cr	Ni-30Cr			8	.000100	$150 \times 10^{-6}$	$.015 \times 10^{-6}$	2.0	.000050	30.0
Rhodium	Rh	+13.4	2239K			$4.5 \times 10^{-6}$				.9

\*NASA Pd-13Cr cast ribbon 10-17-86

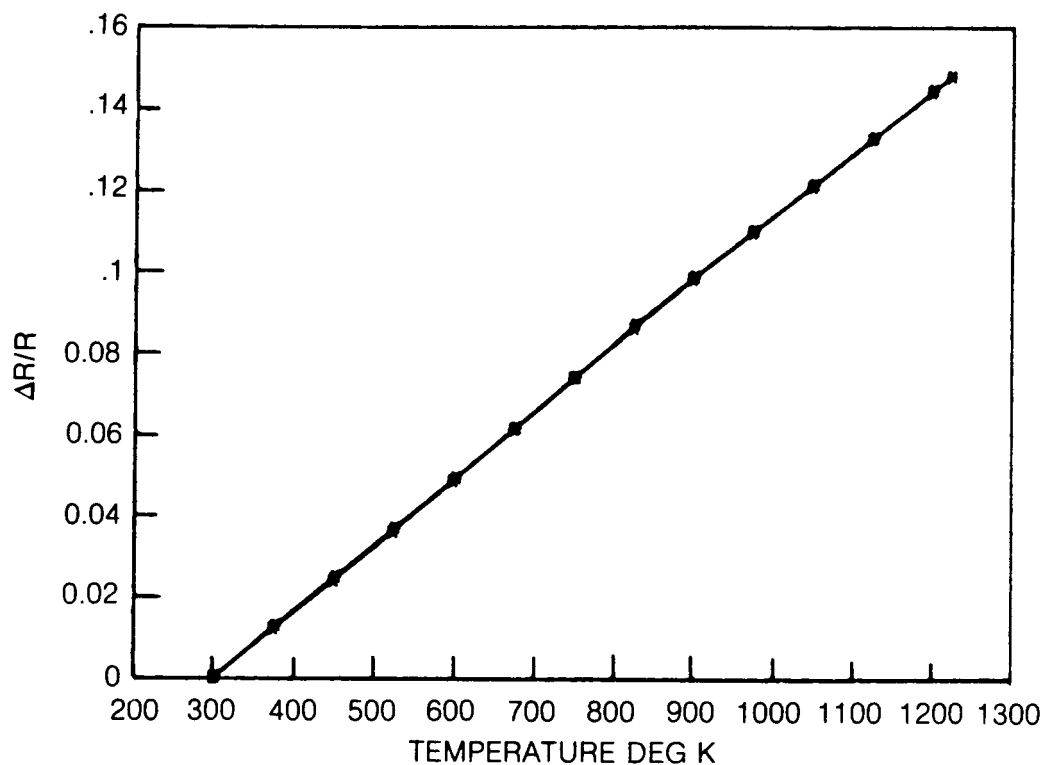


Figure 1. Resistance vs Temperature at 50 deg K/min (Pd-13 Wt % Cr)

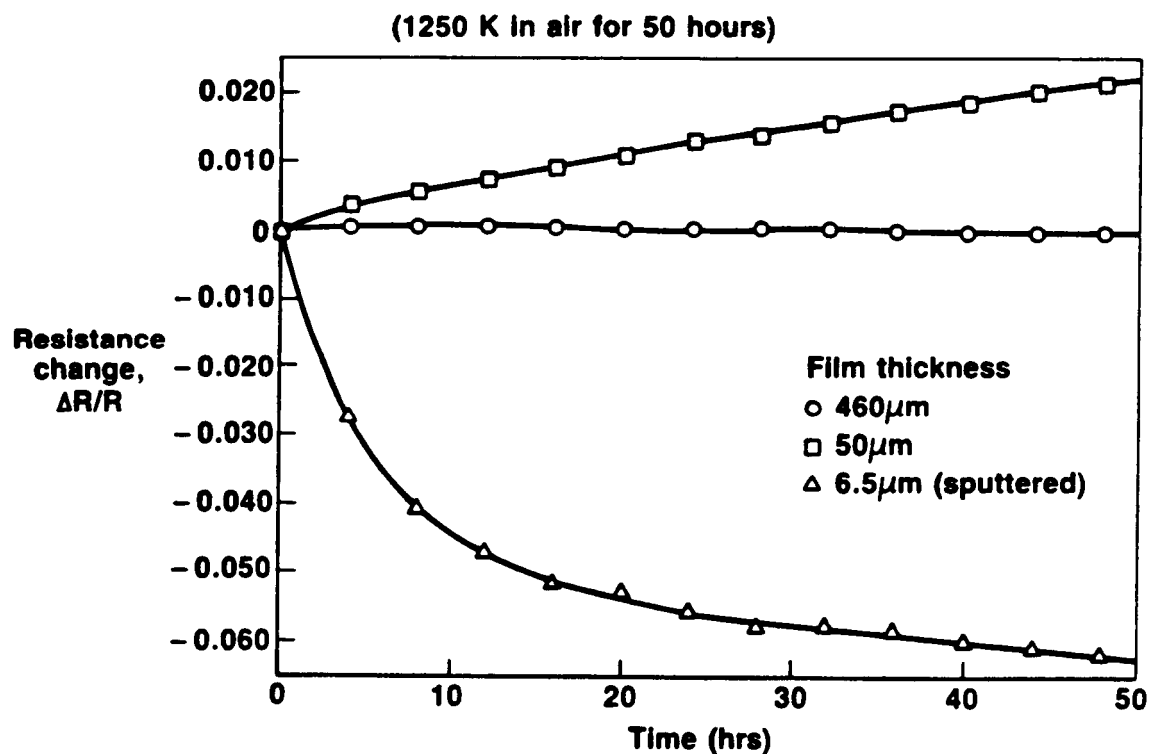
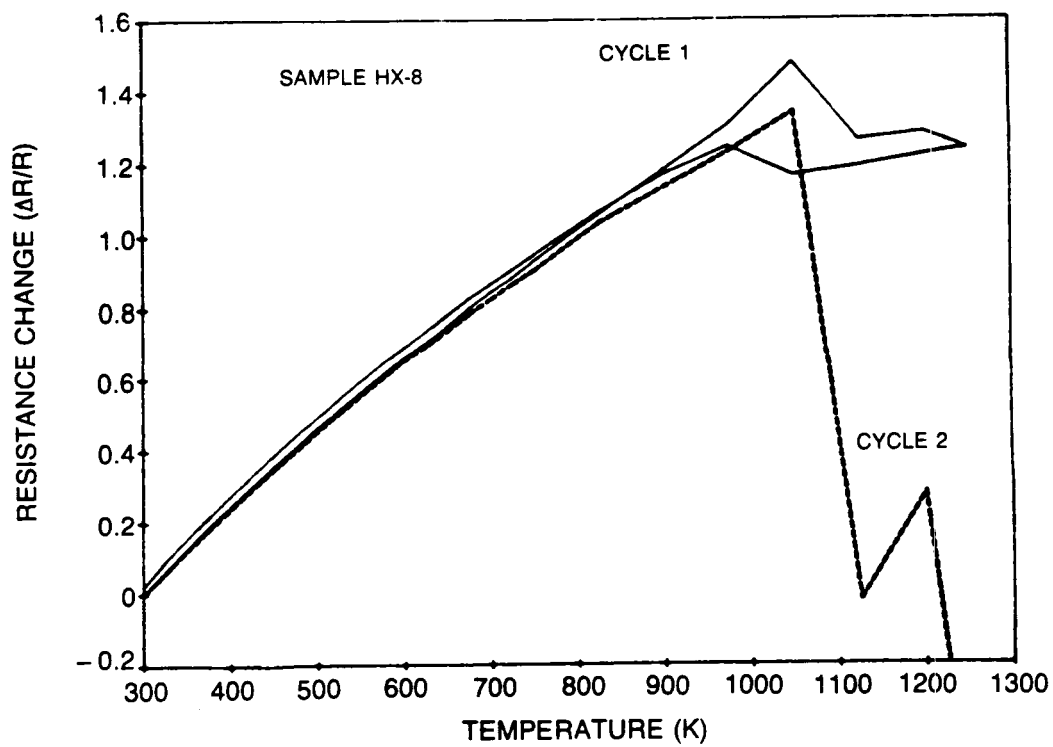
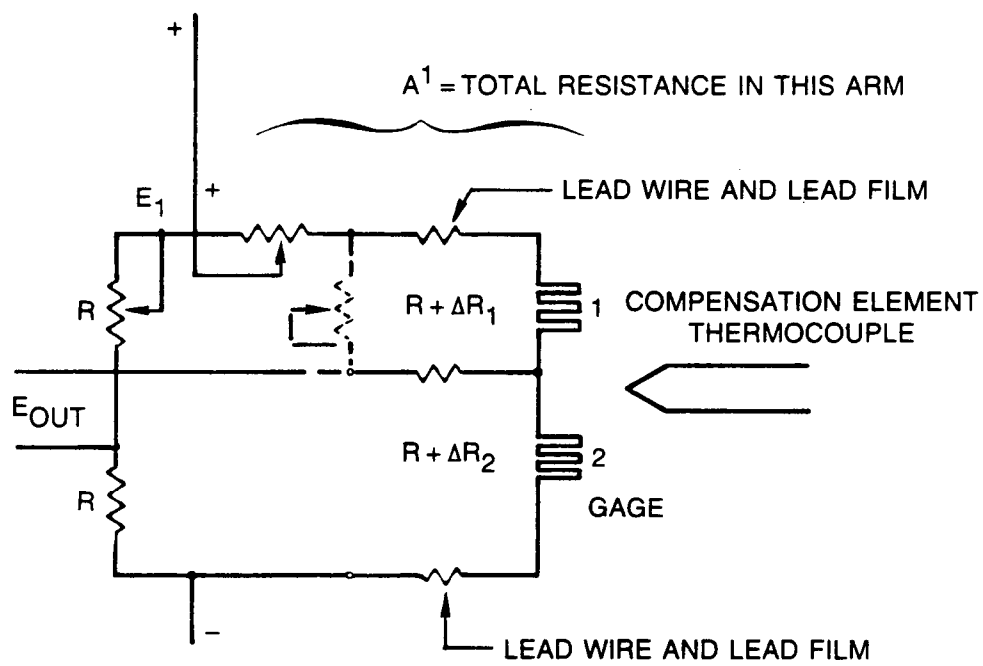


Figure 2. Effect of Film Thickness on Drift in Resistance of Pd-13 wt % Cr



**Figure 3. Resistance vs Temperature for Sputtered Pd-13Cr (wt%) Pretreated 10 hrs in Air at 1370 K**





**Figure 4. Temperature Compensation Arrangements**